Pergamon

PII: S0020–7683(97)00259–X

STRESS INTENSITY FACTORS FOR INTER-LAMINAR CRACKED COMPOSITES UNDER ARBITRARY NORMAL CRACK SURFACE LOADING

SUNG HO KIM†

Agency for Defense Development, Taejeon. Korea

KANG YONG LEE and MOON BOK PARK

Department of Mechanical Engineering, Yonsei University, Seoul, Korea

Abstract— A model is constructed to evaluate the stress intensity factors (SIFs) for composites with an inter-laminar crack subjected to an arbitrary normal loading. A mixed boundary value problem is formulated by the Fourier integral transform method and a Fredholm integral equation of the first kind is derived. The integral equation is solved numerically. The mode I SIFs are evaluated for various ratios of shear moduli of successive layers and ratios of crack length-to-layer thickness. Furthermore, the terms as well as the shape of crack surface polynomial loading and the number of layers affect the variation of SIFs. © 1998 Elsevier Science Ltd. All rights reserved.

NOMENCLATURE

a	half crack length
$g(x)$	arbitrary crack surface pressure
G_j	Fourier transformation of Airy stress function for the j-th layer
h_j	distance from the crack to the exterior interface of the j-th layer
$J_0(\xi t), J_1(\xi t)$	Bessel function of the first kind of order 0 and 1, respectively.
n	number of layers
p_{2k}, p_{2k-1}	influence coefficients for symmetric and anti-symmetric loading parts, respectively
β	order of each term of polynomial loading
t_f	fiber layer thickness
t_{f1}	first fiber layer thickness
t_{f2}	second fiber layer thickness
t_{m0}	cracked resin layer thickness
t_m	sound resin layer thickness
$W(\tau_m), W(\alpha_l)$	integration weights for Gaussian and Laguerre integrations, respectively
V_{LF}	local fiber volume fraction
V_{GF}	global fiber volume fraction
μ_j	shear modulus for the j-th layer
ν_j	Poisson's ratio for the j-th layer
Γ_j	shear modulus ratio ($\equiv \mu_j/\mu_{j-1}$)
ξ	Fourier transformation variable
$\sigma_{yy(j)}, \sigma_{xy(j)}, \sigma_{xx(j)}$	stress components for the j-th layer
$u_{(j)}, v_{(j)}$	displacement components for the j-th layer
τ_m, α_l	integration abscissas for Gaussian and Laguerre integrations, respectively
$A_j(\xi), B_j(\xi), C_j(\xi), D_j(\xi)$	unknown coefficients

INTRODUCTION

Recently, a lot of papers studied the fracture problem for the layered material weakened by a crack. Gecit and Erdogan (1978), Hilton and Sih (1971), and Fowser and Chou (1991) considered the intra-laminar crack in a layered material under a uniform loading. Hilton and Sih (1970) considered a cracked layer bonded between two half-planes under a uniform loading and derived stress intensity factors (SIFs) by the integral transform method. Delale

---

† Author to whom correspondence should be addressed. Present address: Samsung Motors Inc., Technology Center, San No. 50, Kongse-Ri, Kihung-Eup, Yongin-City, Kyungki-Do, Korea 449-900. Tel.: 0082 331 289 7472. Fax: 0082 331 289 7799. E-mail: ksh0312@samsung.co.kr.

and Erdogan (1988) obtained mode I and mode III SIFs for two homogeneous elastic half planes bonded through a non-homogeneous layer with a central crack. Lin and Keer (1989) solved the problem of a vertical crack being in a multi-layered medium. Also, Kim *et al.* (1991, 1992) faced the problem of cracks being in three-layered elastic medium under in-plane, anti-plane shear and uniform tension loadings, respectively. On the other hand, Isida (1971, 1976) solved a problem for non-uniformly stressed central crack embedded in finite and infinite plates by using Laurent expansions of the complex potentials. Chen (1989) obtained SIFs for the anti-symmetric crack surface loading by the Fourier integral transform method. Chen and Chang (1989) obtained mode I and II SIFs for an infinite plate by an efficient finite element alternating method. Fan and Keer (1990) evaluated mode I and II SIFs for the strip with a semi-infinite crack subjected to an arbitrarily distributed traction on the crack surface. Noda *et al.* (1992) studied SIFs for two bonded elastic layers with a single edge crack under various loading conditions. Recently, Lee *et al.* (1994a) considered the problem of a three-layered material with a cracked layer, which is subjected to normal crack surface tractions linearly varying and evaluated mode I SIF. Also, Kim *et al.* (1995) as well as Lee *et al.* (1994b) studied the cracked multi-layered medium subjected to anti-symmetric normal crack surface tractions.

In this paper, the problem of the inter-laminar cracked composites subjected to an arbitrary crack surface loading normal to the crack axis is studied. Following the linear elasticity approach and using the Fourier integral transform method, a Fredholm integral equation of the first kind is derived and SIFs are evaluated numerically. The obtained values of SIFs are presented for each term of crack surface polynomial loading, the number of layers, the ratio of shear moduli between successive layers, Poisson's ratio, ratio of the crack length-to-layer thickness and the thickness of each layer. Furthermore, SIFs for E-glass/epoxy composites as well as the hybrid composites are evaluated as a frequently encountered composites in practical applications.

PROBLEM FORMULATION

Consider a plane-strain type layered material with a central crack subjected to arbitrary surface loadings as illustrated in Fig. 1. It is assumed that the crack is parallel to the layers interface, whereas the successive isotropic layers consist of different materials are perfectly bonded to one another. Using the Fourier integral transformation, stress and displacement components can be formulated for symmetric and anti-symmetric loadings, respectively, in the form

$$\sigma_{xx(j)} = \frac{1}{\pi} \int_0^\infty \frac{\partial^2 G_j}{\partial y^2} \begin{bmatrix} \cos \xi x \\ \sin \xi x \end{bmatrix} \mathrm{d}\xi$$

$$\sigma_{yy(j)} = \frac{-1}{\pi} \int_0^\infty \xi^2 G_j \begin{bmatrix} \cos \xi x \\ \sin \xi x \end{bmatrix} \mathrm{d}\xi$$

$$\sigma_{xy(j)} = \frac{1}{\pi} \int_0^\infty \xi \frac{\partial G_j}{\partial y} \begin{bmatrix} \sin \xi x \\ -\cos \xi x \end{bmatrix} \mathrm{d}\xi$$

$$u_{(j)} = \frac{(1+v_j)}{\pi E_j} \int_0^\infty \left[(1-v_j)\frac{\partial^2 G_j}{\partial y^2} + v_j \xi^2 G_j \right] \begin{bmatrix} \sin \xi x \\ -\cos \xi x \end{bmatrix} \mathrm{d}\xi/\xi$$

$$v_{(j)} = \frac{(1+v_j)}{\pi E_j} \int_0^\infty \left[(1-v_j)\frac{\partial^3 G_j}{\partial y^3} + (v_j-2)\xi^2 \frac{\partial G_j}{\partial y} \right] \begin{bmatrix} \cos \xi x \\ \sin \xi x \end{bmatrix} \mathrm{d}\xi/\xi^2 \tag{1}$$
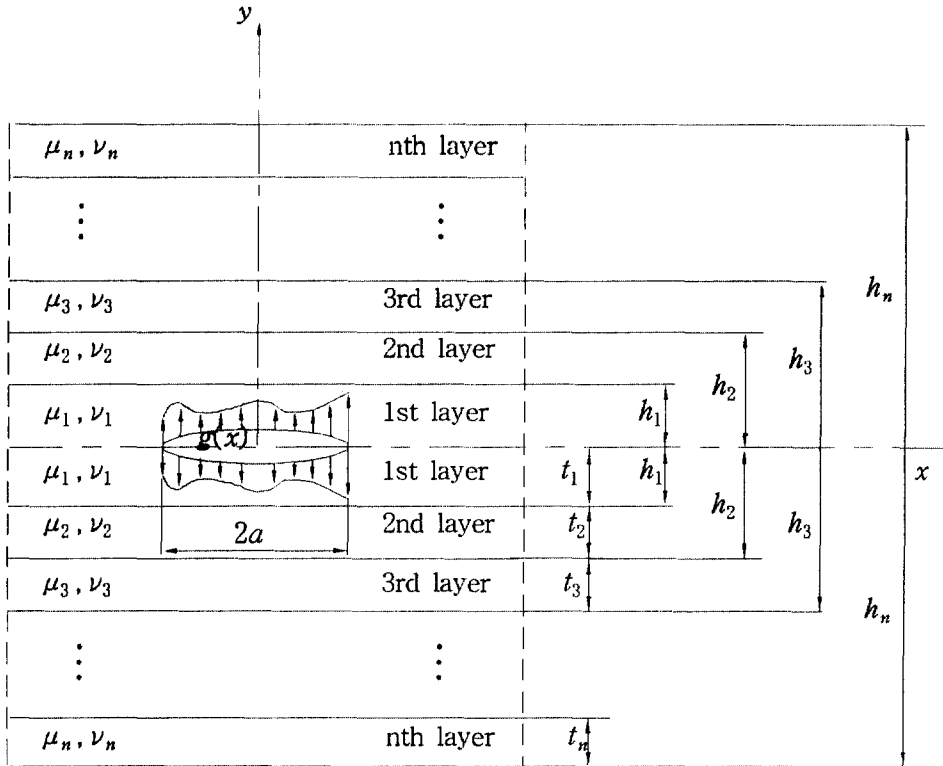
where

Fig. 1. Configuration of the model.

$$G_j = [A_j(\xi) + \xi y B_j(\xi)]\cosh(\xi y) + [C_j(\xi) + \xi y D_j(\xi)]\sinh(\xi y) \quad (j = 1, 2, 3, \ldots, n) \quad (2)$$

The subscript $j = 1$ represents the first layer where the crack is located. It is assumed that the thickness of the layers is identical, v_j and E_j are Poisson's ratio and Young's modulus for the j-th layer, respectively. The unknown coefficients $A_j(\xi)$, $B_j(\xi)$, $C_j(\xi)$ and $D_j(\xi)$ are to be determined.

Because of the symmetry of the configuration for the considered model in relation to the crack axis, just the upper half plane needs to be examined for solving the stated problem. Then, the boundary conditions are as follows:

$$\sigma_{yy(1)} = -g(x) \quad -a < x < a, \quad y = 0$$

$$v_{(1)} = 0 \quad |x| > a, \quad y = 0$$

$$\sigma_{xy(1)} = 0 \quad -\infty < x < \infty, \quad y = 0$$

$$\sigma_{xy(j)} = \sigma_{xy(j-1)} \quad -\infty < x < \infty, \quad y = h_j \quad (j = 1, \ldots, n-1)$$

$$\sigma_{yy(j)} = \sigma_{yy(j+1)} \quad -\infty < x < \infty, \quad y = h_j \quad (j = 1, \ldots, n-1)$$

$$u_{(j)} = u_{(j-1)} \quad -\infty < x < \infty, \quad y = h_j \quad (j = 1, \ldots, n-1)$$

$$v_{(j)} = v_{(j-1)} \quad -\infty < x < \infty, \quad y = h_j \quad (j = 1, \ldots, n-1)$$

$$\sigma_{xy(n)} = 0 \quad -\infty < x < \infty, \quad y = h_n$$

$$\sigma_{yy(n)} = 0 \quad -\infty < x < \infty, \quad y = h_n \quad (3)$$

The arbitrary crack surface pressure $g(x)$ is defined as

$$g(x) = \sum_{\beta=0}^{\infty} p_\beta \left(\frac{x}{a}\right)^\beta = \sum_{k=0}^{\infty} p_{2k} \left(\frac{x}{a}\right)^{2k} + \sum_{k=1}^{\infty} p_{2k-1} \left(\frac{x}{a}\right)^{2k-1} \tag{4}$$

where p_{2k} and p_{2k-1} are the influence coefficients given for the symmetric and anti-symmetric loading parts, respectively.

For simplicity of the formulation, the arbitrary crack surface pressure $g(x)$ is separated into symmetric and anti-symmetric loading parts without loss of generality. By applying eqns (1b) and (1e) in eqns (3a) and (3b), respectively, the following pair of dual integral equations can be obtained for each loading part.

$$\int_0^\infty M(\xi) \begin{bmatrix} \cos \xi x \\ \sin \xi x \end{bmatrix} d\xi = \begin{bmatrix} 0 \\ 0 \end{bmatrix} \quad (|x| > a) \tag{5}$$

$$\int_0^\infty \xi F(\xi) M(\xi) \begin{bmatrix} \cos \xi x \\ \sin \xi x \end{bmatrix} d\xi = \pi \begin{bmatrix} p_{2k} \left(\dfrac{x}{a}\right)^{2k} \\ \\ p_{2k-1} \left(\dfrac{x}{a}\right)^{2k-1} \end{bmatrix} \quad (|x| < a) \tag{6}$$

where

$$F(\xi) \equiv \frac{\xi A_1(\xi)}{M(\xi)} \tag{7}$$

$$M(\xi) \equiv \xi B_1(\xi) \tag{8}$$

$$B_1(\xi) = -C_1(\xi) \tag{9}$$

Furthermore, $A_1(\xi)$ can be defined as follows:

$$T = \tilde{Q}^{-1} R \tag{10}$$

where

$$T = [A_1, D_1, A_2, B_2, C_2, D_2, \ldots, A_n, B_n, C_n, D_n]^T \tag{11}$$

$$R = [R_1, R_2, R_3, R_4, \ldots, R_{4n-2}]^T \tag{12}$$

$$R_1 = \tanh z_1 - z_1, \quad R_2 = -z_1 \tanh z_1, \quad R_3 = -[(1 - 2v_1) \tanh z_1 + z_1],$$
$$R_4 = z_1 \tanh z_1 - 2(1 - v_1), \quad R_5 = R_6 = \cdots = R_{4n-2} = 0 \quad (z_1 \equiv \xi h_1) \tag{13}$$

and $\tilde{Q}$ is defined in the Appendix.

By following the method of Copson (1961), $M(\xi)$ is defined for symmetric and anti-symmetric loading problems, respectively, in the form

$$M(\xi) = \int_0^a \begin{bmatrix} \phi_{2k}(t) J_0(\xi t) \\ \psi_{2k-1}(t) J_1(\xi t) \end{bmatrix} dt \tag{14}$$

where J_0 and J_1 are the Bessel function of the first kind of order 0 and 1, respectively, whereas $\phi_{2k}(t)$ and $\psi_{2k-1}(t)$ are to be determined. By taking into account eqn (14), eqn (5) is automatically satisfied and eqn (6) is reduced to the form of the Fredholm integral equation of the second kind as follows:

$$\begin{bmatrix} \Phi_{2k}(\sigma) \\ \Psi_{2k-1}(\sigma) \end{bmatrix} + \int_0^1 K(\tau,\sigma) \begin{bmatrix} \Phi_{2k}(\tau) \\ \Psi_{2k-1}(\tau) \end{bmatrix} d\tau = \begin{bmatrix} q_{2k}(\sigma) \\ f_{2k-1}(\sigma) \end{bmatrix} \qquad (15)$$

where

$$K(\tau,\sigma) = \sqrt{\tau\sigma} \int_0^\infty \alpha[F(\alpha/a)-1] \begin{bmatrix} J_0(\alpha\tau)J_0(\alpha\sigma) \\ J_1(\alpha\tau)J_1(\alpha\sigma) \end{bmatrix} d\alpha$$

$$q_{2k}(\sigma) = \frac{(2k-1)!!}{(2k)!!} \sigma^{2k+1/2}$$

$$f_{2k-1}(\sigma) = \frac{(2k-1)!!}{(2k)!!} \sigma^{2k-1/2}$$

$$(2k-1)!! \equiv (2k-1) \times (2k-3), \dots, 3 \times 1, \quad (2k)!! \equiv (2k) \times (2k-2), \dots, 4 \times 2$$

$$t \equiv a\tau, \quad s \equiv a\sigma, \quad \alpha \equiv \xi a, \quad x \equiv a\bar{x}$$

$$\phi_{2k}(t) \equiv \pi\sqrt{a\alpha}p_{2k}\Phi_{2k}(\tau), \quad \psi_{2k-1} \equiv \pi\sqrt{a\alpha}p_{2k-1}\Psi_{2k-1}(\tau) \qquad (16)$$

To solve the Fredholm integral equation, the Gaussian–Laguerre integration technique is utilized. At $\tau_m = \sigma_m$ $(m = 1 \sim N_G)$, $\Phi_{2k}(\tau_m)$ and $\Psi_{2k-1}(\tau_m)$ can be determined numerically as follows:

$$\sum_{m=1}^{N_G} \left\{ \delta_{me} + K(\tau_m,\tau_e) \begin{bmatrix} \Phi_{2k}(\tau_m) \\ \Psi_{2k-1}(\tau_m) \end{bmatrix} W(\tau_m) \right\} = \begin{bmatrix} q_{2k}(\tau_e) \\ f_{2k-1}(\tau_e) \end{bmatrix} \quad (e = 1 \sim N_G) \qquad (17)$$

$$K(\tau_m,\tau_e) = \sqrt{\tau_m\tau_e} \sum_{l=1}^{N_l} \alpha_l[F(\alpha_l/a)-1] \begin{bmatrix} J_0(\alpha_l t_m)J_0(\alpha_l\tau_e) \\ J_1(\alpha_l\tau_m)J_1(\alpha_l\tau_e) \end{bmatrix} W(\alpha_l) \qquad (18)$$

where δ_{me} is Kronecker's delta, τ_m and α_l are the abscissas for Gaussian and Laguerre integrations, respectively, and τ_e is the collocation point. $W(\alpha_l)$ and $W(\tau_m)$ are the weight factors for Laguerre and Gaussian integrations, respectively, with N_l and N_G being the number of integration points. The SIFs for both sides of the crack tips are calculated in the forms

$$K_{IR} = \lim_{\bar{x} \to 1^-} \sqrt{2\pi a(\bar{x}-1)}\sigma_{yy(1)}(\bar{x},0)$$

$$K_{IL} = \lim_{\bar{x} \to -1^-} \sqrt{-2\pi a(\bar{x}+1)}\sigma_{yy(1)}(\bar{x},0) \qquad (19)$$

where K_{IR} and K_{IL} represent SIFs at the right and left-hand side crack tip, respectively. After some integral manipulations for $\sigma_{yy(1)}(\bar{x},0)$, the SIFs are obtained in the forms

$$K_{IR} = \sqrt{\pi a} \left[\Phi_0(1)p_0 + \sum_{k=1}^\infty \{\Phi_{2k}(1)p_{2k} + \Psi_{2k-1}(1)p_{2k-1}\} \right]$$

$$K_{IL} = \sqrt{\pi a} \left[\Phi_0(1)p_0 + \sum_{k=1}^\infty \{\Phi_{2k}(1)p_{2k} - \Psi_{2k-1}(1)p_{2k-1}\} \right] \qquad (20)$$

NUMERICAL RESULTS AND DISCUSSION

For the homogeneous isotropic half space case, the kernel $K(\tau,\sigma)$ in eqn (15) approaches zero because $F(\alpha/a) = 1$. Therefore, the SIFs are obtained explicitly as follows:

$$K_{\mathrm{IR}} = \sqrt{\pi a}\left[p_0 + \sum_{k=1}^{\infty} \frac{(2k-1)!!}{(2k)!!}\{p_{2k}+p_{2k-1}\} \right] = \left(p_0 + \frac{1}{2}p_1 + \frac{1}{2}p_2 + \frac{3}{8}p_3 + \cdots \right)\sqrt{\pi a}$$

$$K_{\mathrm{IL}} = \sqrt{\pi a}\left[p_0 + \sum_{k=1}^{\infty} \frac{(2k-1)!!}{(2k)!!}\{p_{2k}-p_{2k-1}\} \right] = \left(p_0 - \frac{1}{2}p_1 + \frac{1}{2}p_2 - \frac{3}{8}p_3 + \cdots \right)\sqrt{\pi a} \qquad (21)$$

The results coincide with those obtained in the works of Isida (1971, 1976), Tada *et al.* (1973) and Chen (1989).

For simplicity of the analysis in the three-layered material case, it is assumed that each layer is composed of identical thicknesses ($t_1 = t_2 = t_3 = t_0$). In earlier studies, Kim *et al.* (1991) showed that the Poisson's ratio does not significantly influence SIFs, and therefore, the Poisson's ratio for each layer is assumed as 0.3. Figure 2 shows the dimensionless SIFs for each term (β) of polynomial loading, $K_{\mathrm{I}}^{(\beta)}/(p_\beta\sqrt{\pi a})$, in the right crack tip with the variations of crack length-to-layer thickness ratio (a/t_0) and shear modulus ratio. The dimensionless SIF increases as the a/t_0 increases. (Actual SIFs increase as the width of the cracked layer, t_0 decreases when the crack length, a, is fixed.) The dimensionless SIFs for layered material with $\Gamma_1 = \Gamma_2 = 2.0$ are higher than those obtained with $\Gamma_1 = \Gamma_2 = 0.5$. Also, the dimensionless SIFs greatly reduce as discussed by Isida (1976) and Lee *et al.* (1994) as the order (β) of each term of polynomial loading increases when the even and odd terms of the polynomial are considered separately. The convergencies of the solutions are examined in Table 1 and the accuracy needed in the engineering viewpoint is acquired.

Next, the multi-layer case is considered. For simplicity of the problem, it is assumed that each layer is composed of identical thickness ($t_1 = t_2 = \cdots = t_n = t_0$) and the shear moduli of the layers are gradually increasing or decreasing. As shown in Fig. 3, the
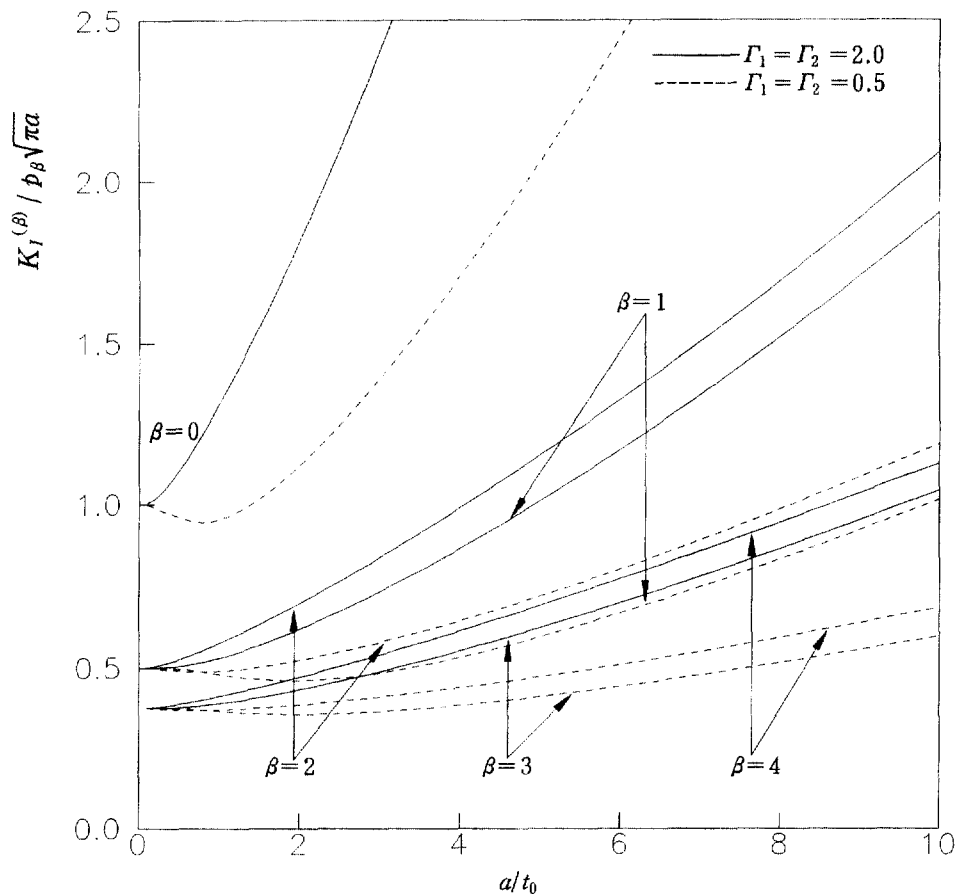

Fig. 2. Dimensionless stress intensity factor for a three-layered case.

Table 1. Convergency of numerical analysis for dimensionless stress intensity factor

N_i	N_G	$\Gamma_1 = \Gamma_2 = 0.5$ $a/t_0 = 0.1$ $\beta = 0$	$\Gamma_1 = \Gamma_2 = 0.2$ $a/t_0 = 4.0$ $\beta = 0$	$\Gamma_1 = \Gamma_2 = 0.5$ $a/t_0 = 4.0$ $\beta = 1$	$\Gamma_1 = \Gamma_2 = 0.2$ $a/t_0 = 4.0$ $\beta = 1$
10	50	0.993726	3.056173	0.499997	0.876375
	100	0.993726	3.053153	0.499992	0.876374
	110	0.993726	3.053152	0.499992	0.876374
20	50	0.998311	3.052824	0.499995	0.865089
	100	0.998310	3.052810	0.499993	0.865088
	110	0.998310	3.052809	0.499993	0.865088
30	50	0.999030	3.057252	0.499993	0.863858
	100	0.999030	3.057237	0.499993	0.863858
	110	0.999030	3.057237	0.499993	0.863858
40	50	0.998230	3.057372	0.499993	0.863857
	100	0.998230	3.057357	0.499991	0.863830
	110	0.998230	3.057357	0.499991	0.863830

Header: Dimensionless SIFs $(K_1^{(\beta)}/p_\beta\sqrt{\pi a})$

dimensionless SIF for each term of polynomial loading increases as a/t_0 increases, the shear modulus ratio increases and β decreases, as discussed in the previously considered problem of the three-layered material. When the layer is relatively thin $(a/t_0 = 4.0)$, the dimensionless SIF decreases abruptly as the number of layers (n) increases.

For E-glass/epoxy composites shown in Fig. 4, the shear moduli of E-glass fiber and epoxy are 4.4×10^6 psi and 0.19×10^6 psi with Poisson's ratios being 0.2 and 0.35, respectively (Schwartz, 1992). The local fiber volume fraction near the cracked epoxy layer region, V_{LF}, is calculated as (Bechel and Kaw, 1994),

$$V_{LF} = \frac{t_f}{t_{m0} + t_f} \tag{22}$$

Also, the global fiber volume fraction far from the cracked epoxy layer region, V_{GF}, is calculated as

$$V_{GF} = \frac{t_f}{t_m + t_f} \tag{23}$$

In the following numerical analysis, V_{LF} was selected V_{LF} to be equal with 0.2, 0.4, 0.6 and 0.8, whereas V_{GF} takes the values 0.3, 0.5, 0.8 and a/t_{m0} varies from 0.1–4.0. Figure 5 and Table 2 show the dimensionless SIFs for each term $(\beta = 0, 1)$ of polynomial loading in cases of various local and global fiber volume fractions. The dimensionless SIFs depend more on the local fiber volume fraction (V_{LF}) than the global fiber volume fraction (V_{GF}). For the lower local fiber volume fractions, relatively larger dimensionless SIFs are produced. The global fiber volume fraction (V_{GF}), however, contributes significantly to the dimensionless SIFs as the cracked epoxy layer gets thinner $(a/t_{m0} > 2)$ and the local fiber volume fraction is low enough $(V_{LF} = 0.2)$. It is noted that the curves for the dimensionless SIFs attained for the linear crack surface loading case $(\beta = 1)$ present similar trends, whereas their values are smaller than those obtained for the uniform crack surface loading $(\beta = 0)$.

Finally, the hybrid composites case shown in Fig. 6 is considered. The local fiber volume fraction near the cracked epoxy layer region, V_{LF}, is calculated as

(a)

(b)
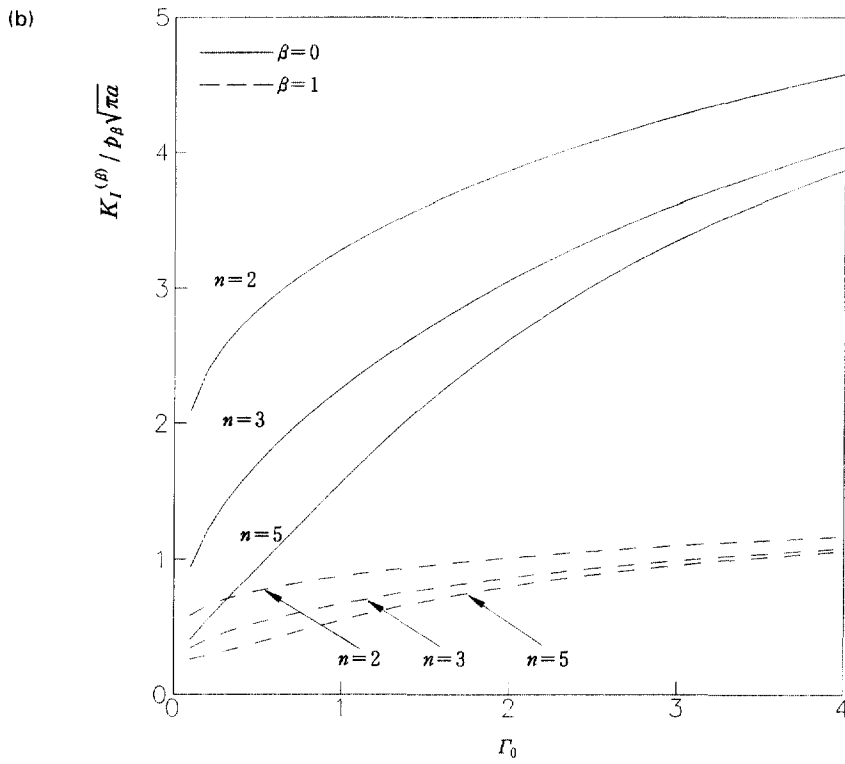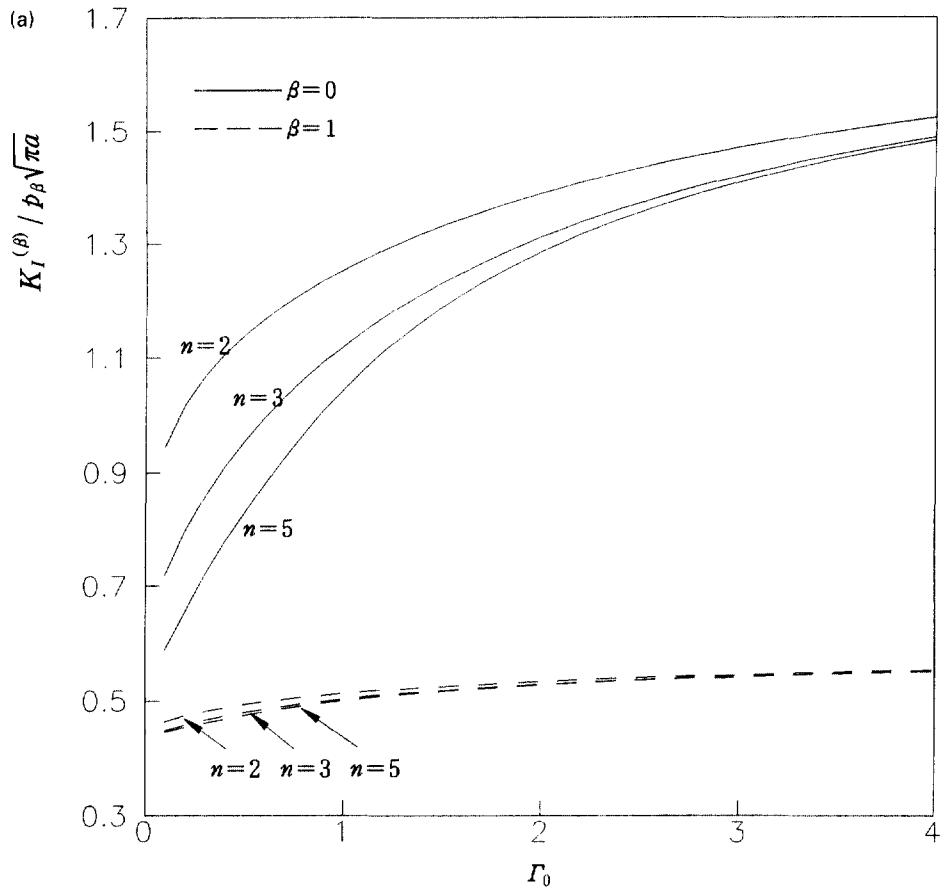
(*b*) $a/t_0 = 4.0$

Fig. 3. Dimensionless stress intensity factor for a multi-layer case. (a) $a/t_0 = 1.0$. (b) $a/t_0 = 4.0$.
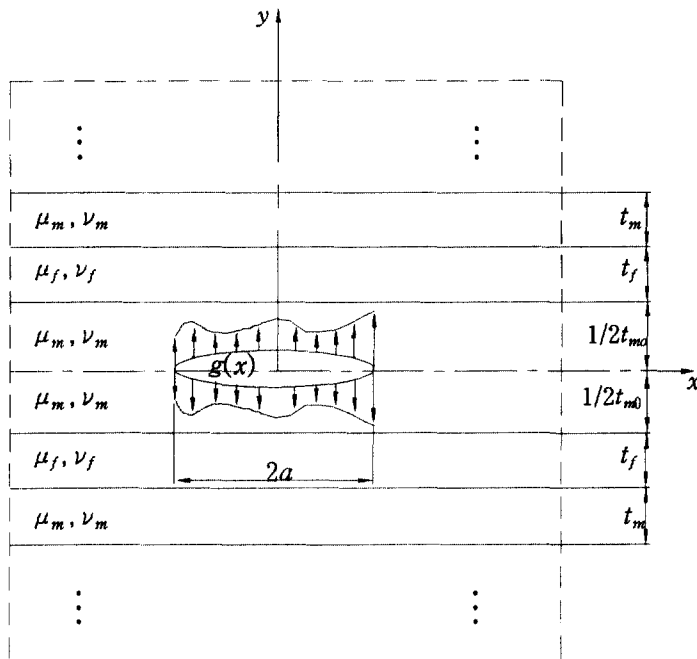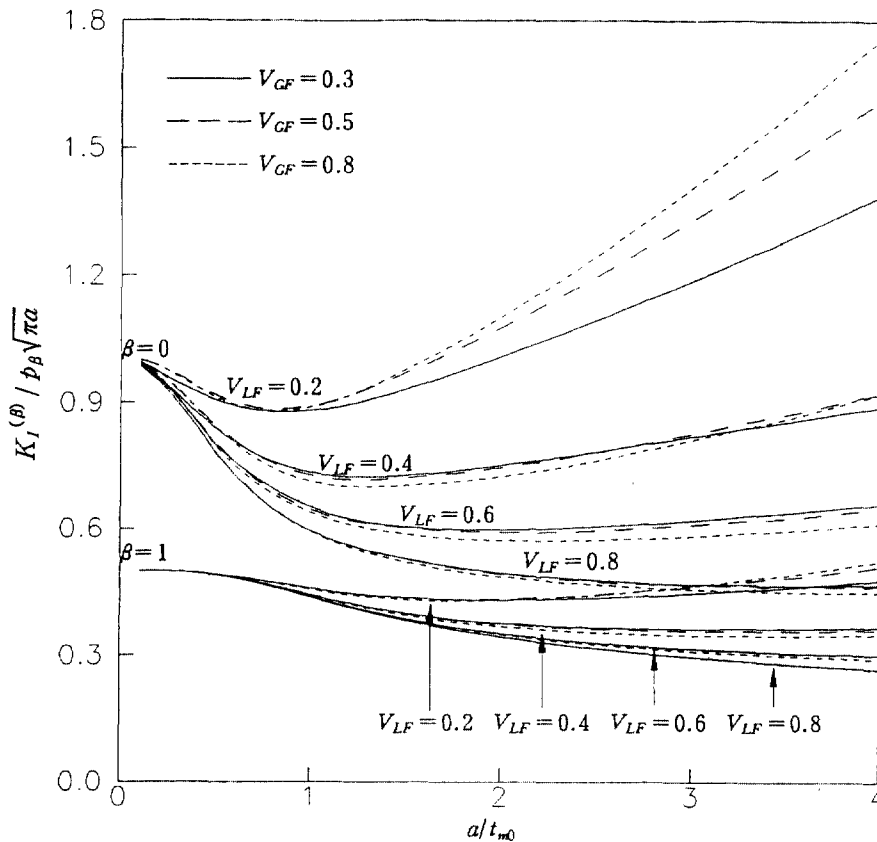
Fig. 4. Geometry of monolithic composites.

Fig. 5. Dimensionless stress intensity factor for E-glass/epoxy composites.

Table 2. Dimensionless stress intensity factor for E-glass/epoxy composites

|	a/t_{m0}	$V_{GF} = 0.3$			$V_{GF} = 0.5$			$V_{GF} = 0.8$		
		$V_{LF} =$ 0.2	$V_{LF} =$ 0.4	$V_{LF} =$ 0.8	$V_{LF} =$ 0.2	$V_{LF} =$ 0.4	$V_{LF} =$ 0.8	$V_{LF} =$ 0.2	$V_{LF} =$ 0.4	$V_{LF} =$ 0.8
$\beta = 0$	0.1	0.998	0.995	0.984	0.998	0.995	0.984	0.998	0.995	0.984
	0.5	0.910	0.844	0.782	0.913	0.839	0.781	0.909	0.833	0.779
	1.0	0.880	0.735	0.595	0.895	0.729	0.595	0.892	0.715	0.593
	2.0	1.101	0.751	0.496	1.108	0.745	0.493	1.110	0.724	0.486
	3.0	1.119	0.818	0.469	1.133	0.825	0.466	1.140	0.810	0.456
	4.0	1.139	0.889	0.468	1.161	0.922	0.464	1.176	0.920	0.449
$\beta = 1$	0.1	0.499	0.499	0.499	0.499	0.499	0.499	0.499	0.499	0.499
	0.5	0.492	0.491	0.490	0.492	0.490	0.490	0.492	0.490	0.490
	1.0	0.459	0.444	0.438	0.458	0.443	0.438	0.456	0.442	0.438
	2.0	0.432	0.377	0.344	0.433	0.374	0.344	0.430	0.368	0.344
	3.0	0.447	0.363	0.296	0.462	0.358	0.296	0.464	0.348	0.295
	4.0	0.479	0.368	0.269	0.511	0.362	0.269	0.523	0.351	0.268
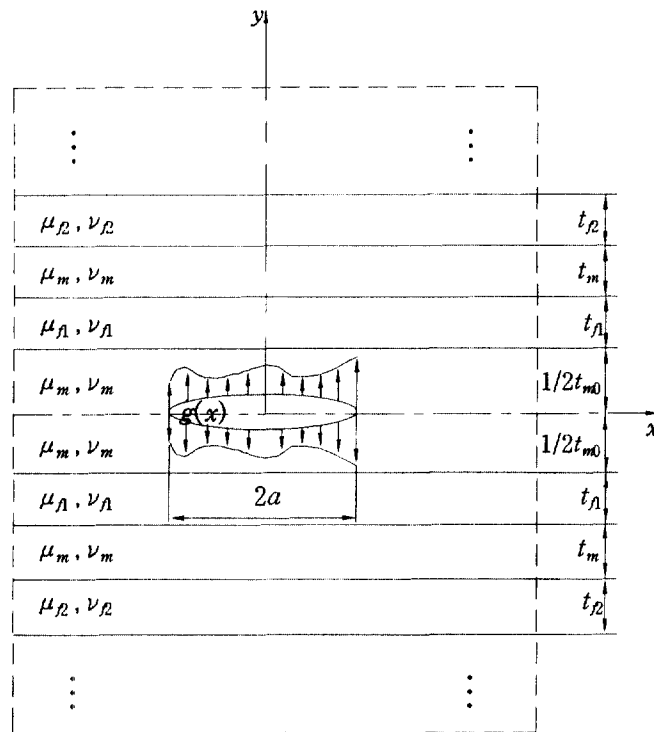
Fig. 6. Geometry of hybrid composites.

$$V_{LF} = \frac{t_{f1}}{t_{m0} + t_{f1}} \tag{24}$$

Also, the global fiber volume fraction far from the cracked epoxy layer region, V_{GF}, is calculated as

$$V_{GF} = \frac{t_{f1} + t_{f2}}{2t_m + t_{f1} + t_{f2}} \tag{25}$$

In the numerical analysis, the shear modulus of graphite fiber is assumed to be 33.3×10^6 psi with Poisson's ratio being 0.2 (Schwartz, 1992). Dimensionless SIFs are tabulated in

Table 3. Dimensionless stress intensity factors for hybrid composites ($V_{GF} = 0.5$)

Composites	V_{LF}	a/t_{m0}					
		0.1	0.5	1.0	2.0	3.0	4.0
(a) $\beta = 0$							
E-glass/epoxy/graphite/epoxy	0.2	0.997	0.894	0.843	0.962	1.116	1.139
	0.5	0.991	0.816	0.671	0.631	0.654	0.688
	0.8	0.984	0.779	0.594	0.492	0.462	0.459
Graphite/epoxy/E-glass/epoxy	0.2	0.995	0.873	0.814	0.949	1.116	1.128
	0.5	0.984	0.773	0.610	0.539	0.553	0.591
	0.8	0.981	0.747	0.535	0.409	0.369	0.349
Graphite/epoxy	0.2	0.995	0.864	0.786	0.883	1.105	1.124
	0.5	0.984	0.772	0.603	0.529	0.536	0.564
	0.8	0.981	0.746	0.535	0.409	0.367	0.347
(b) $\beta = 1$							
E-glass/epoxy/graphite/epoxy	0.2	0.499	0.491	0.454	0.413	0.424	0.458
	0.5	0.499	0.490	0.440	0.359	0.329	0.319
	0.8	0.499	0.490	0.438	0.344	0.296	0.269
Graphite/epoxy/E-glass/epoxy	0.2	0.499	0.490	0.446	0.399	0.414	0.452
	0.5	0.499	0.489	0.433	0.337	0.294	0.276
	0.8	0.499	0.489	0.432	0.329	0.275	0.242
Graphite/epoxy	0.2	0.499	0.495	0.444	0.390	0.394	0.422
	0.5	0.499	0.489	0.433	0.337	0.293	0.274
	0.8	0.499	0.489	0.432	0.329	0.274	0.242

Table 3 for various composites with $V_{GF} = 0.5$. The effect of V_{LF} on dimensionless SIFs for various composites, is similar with that for E-glass/epoxy composites.

CONCLUSIONS

The SIFs for a central crack subjected to arbitrary normal loadings in a multi-layered material, which is composed of elastically dissimilar layer, was analyzed by the Fourier integral transform method. The following conclusions are obtained from the numerical analysis.

(1) The dimensionless SIFs for the half space case and the three-layered material case agree with the previous results.
(2) For the multi-layered material, the dimensionless SIFs for each term of polynomial loading increase as the crack length-to-layer thickness ratio and ratio of shear moduli of the successive layers increase, and as the order of each term of polynomial loading and the number of layers decrease.
(3) For monolithic and hybrid composites, the dimensionless SIFs for each term of polynomial loading depend mainly on the local fiber volume fractions. As the local fiber volume fraction decreases, SIFs increase.

REFERENCES

Bechel, V. T. and Kaw, A. K. (1994) Fracture mechanics of composites with nonhomogeneous interphases and nondilute fiber volume fractions. *International Journal of Solids and Structures* **31**(15), 2053–2070.
Chen, Y. Z. (1989) Crack problem in plane elasticity under antisymmetric loading. *International Journal of Fracture* **41**, R29–R34.
Chen, W. H. and Chang, C. S. (1989) Analysis of two-dimensional fracture problems with multiple cracks under mixed boundary conditions. *Engineering Fracture Mechanics* **34**(4), 921–934.
Copson, E. T. (1961) On certain dual integral equations. *Proceedings of the Glasgow Mathematical Association* **5**, 19–24.
Delale, F. and Erdogan, F. (1988) On the mechanical modeling of the interfacial region in bonded half-planes. *ASME Journal of Applied Mechanics* **55**, 317–324.
Fan, H. and Keer, L. M. (1990) Two-dimensional contact on an anisotropic elastic half-space. *ASME Journal of Applied Mechanics* **61**, 250–255.
Fowser, S. W. and Chou, T. W. (1991) Integral equations solution for reinforced mode I cracks opened by internal pressure. *ASME Journal of Applied Mechanics* **58**, 464–472.

Gecit, M. R. and Erdogan, F. (1978) The effect of adhesive layers on the fracture of laminated structures. *ASME Journal of Engineering Materials and Technology* **100**, 2–9.

Hilton, P. D. and Sih, G. C. (1970) A sandwiched layer of dissimilar material weakened by crack like imperfections. *Proceedings of the Fifth South Eastern Conference on the Theoretical and Applied Mechanics*, ed. G. L. Rogers, S. C. Kranc and E. G. Henneke, **5**, 123–149.

Hilton, P. D. and Sih, G. C. (1971) A laminated composite with a crack normal to the interface. *International Journal of Solids and Structures* **7**, 913–930.

Isida, M. (1971) Effect of width and length on stress intensity factors of internally cracked plates under various boundary conditions. *International Journal of Fracture* **7**(3), 301–316.

Isida, M. (1976) Elastic analysis of cracks and stress intensity factors (in Japanese). *Fracture Mechanics and Strength of Materials* **2**, 128. Baifuukan.

Kim, S. H., Oh, J. H. and Ong, J. W. (1991) Stress intensity factors for a center cracked laminated composites under uni-axial tension (in Korean). *The Korean Society of Mechanical Engineers* **15**(5), 1611–1619.

Kim, S. H., Oh, J. H. and Ong, J. W. (1992) Stress intensity factors for a center cracked laminated composites under shear loading (in Korean). *The Korean Society of Mechanical Engineers* **16**(5), 838–848.

Kim, S. H., Lee, K. Y. and Park, M. B. (1995) Mode I stress intensity factors for layered materials under anti-symmetric loading. *Engineering Fracture Mechanics* **51**(5), 837–846.

Lee, K. Y., Park, M. B. and Kim, S. H. (1994a) Stress intensity factors for layered material under anti-symmetric loading (in Korean). *The Korean Society of Mechanical Engineers* **18**(6), 1382–1387.

Lee, K. Y., Kim, S. H. and Park, M. B. (1994b) Stress intensity factors for multi-layered material under anti-symmetric polynomial loading (in Korean). *The Korean Society of Mechanical Engineers*, in press.

Lin, W. and Keer, L. M. (1989) Analysis of a vertical crack in a multi-layered medium. *ASME Journal of Applied Mechanics* **56**, 63–69.

Noda, N. A., Araki, K. and Erdogan, F. (1992) Stress intensity factors in two bonded elastic layers with a single edge crack under various loading conditions. *International Journal of Fracture* **31**, 101–126.

Schwartz, M. M. (1992) *Composite Materials Handbook*, 2nd edn. McGraw-Hill.

Tada, H., Paris, P. and Irwin, G. (1973) *The Stress Analysis of Cracks Handbook*. Del Research, Hellertown.

APPENDIX

The components for $\tilde{Q}$ in eqn (10) are defined as follows:

$$Q_{11} = 1$$
$$Q_{12} = z_1 \tanh z_1$$
$$Q_{21} = \tanh z_1$$
$$Q_{22} = \tanh z_1 + z_1$$
$$Q_{31} = 1$$
$$Q_{32} = z_1 \tanh z_1 + 2(1 - v_1)$$
$$Q_{41} = -\tanh z_1$$
$$Q_{42} = (1 - 2v_1) \tanh z_1 - z_1 \tag{A1}$$

$$Q_{(4j-3)(4j-1)} = -1$$
$$Q_{(4j-3)(4j)} = -z_j$$
$$Q_{(4j-3)(4j+1)} = -\tanh z_j$$
$$Q_{(4j-3)(4j+2)} = -z_j \tanh z_j$$
$$Q_{(4j-2)(4j-1)} = -\tanh z_j$$
$$Q_{(4j-2)(4j)} = -z_j \tanh z_j - 1$$
$$Q_{(4j-2)(4j-1)} = -1$$
$$Q_{(4j-2)(4j-2)} = -\tanh z_j - z_j$$
$$Q_{(4j-1)(4j-1)} = -\Gamma_j$$
$$Q_{(4j-1)(4j)} = -\Gamma_j[-2(1 - v_{j+1}) \tanh z_j + z_j]$$
$$Q_{(4j-1)(4j+1)} = -\Gamma_j \tanh z_j$$
$$Q_{(4j-1)(4j+2)} = -\Gamma_j[2(1 - v_j) + z_j \tanh z_j]$$
$$Q_{(4j)(4j-1)} = \Gamma_j \tanh z_j$$
$$Q_{(4j)(4j)} = \Gamma_j[-1 + 2v_{j+1} + z_j \tanh z_j]$$
$$Q_{(4j)(4j+1)} = \Gamma_j$$
$$Q_{(4j)(4j+2)} = \Gamma_j[(2v_{j-1} - 1) \tanh z_j + z_j]$$
$$Q_{(4j+1)(4j-1)} = 1$$

$$Q_{(4j+1)(4j)} = -z_{j+1}$$

$$Q_{(4j+1)(4j+1)} = \tanh z_{j+1}$$

$$Q_{(4j+1)(4j+2)} = z_{j+1} \tanh z_{j+1}$$

$$Q_{(4j+2)(4j-1)} = \tanh z_{j+1}$$

$$Q_{(4j+2)(4j)} = z_{j+1} \tanh z_{j} + 1$$

$$Q_{(4j+2)(4j+1)} = 1$$

$$Q_{(4j+2)(4j+2)} = \tanh z_{j-1} + z_{j-1} \quad (j = 1 \text{ to } n-1) \tag{A2}$$

$$Q_{(4j+3)(4j-1)} = 1$$

$$Q_{(4j-3)(4j)} = 2(1 - v_{j+1}) \tanh z_{j+1} + z_{j+1}$$

$$Q_{(4j+3)(4j+1)} = \tanh z_{j+1}$$

$$Q_{(4j+3)(4j+2)} = z_{j+1} \tanh z_{j+1} + 2(1 - v_{j+1})$$

$$Q_{(4j+4)(4j-1)} = -\tanh z_{j+1}$$

$$Q_{(4j-4)(4j)} = -z_{j+1} \tanh z_{j+1} + 1 - 2v_{j+1}$$

$$Q_{(4j+4)(4j+1)} = -1$$

$$Q_{(4j+4)(4j-2)} = \tanh z_{j+1}(1 - 2v_{j+1}) - z_{j+1} \quad (j = 1 \text{ to } n-2) \tag{A3}$$

where $\Gamma_j \equiv \mu_j/\mu_{j-1}$, $z_j \equiv \zeta h h_j$ ($j = 1$ to $n-1$). All other components are zero.